High Barrier, Biodegradable Nanocomposite Films Based on Clay-Coated and Chemically Modified Gum Kondagogu

Abhilash Venkateshaiah, Renee L. Timmins, Elmar Sehl, Stanisław Wacławek, Miroslav Černík, Vinod V. T. Padil,* and Seema Agarwal*

Lately, environmentally benign packaging materials with biodegradability, flexibility, and high barrier properties are sought after as a substitute for conventional plastic packaging materials due to increasing plastic pollution and microplastics in the environment. Although natural polymers can be sustainable alternatives to petro-sourced, non-biodegradable plastics, they suffer from the poor barrier and mechanical properties. In this study, a mechanically stable, biodegradable film of tree gum kondagogu with remarkable barrier properties is fabricated. The introduction of spray-coated, waterborne, large-aspect ratio sodium-hectorite dispersion on tree-gum films ensured very high barrier properties even at high relative humidity conditions (oxygen transmission rate (OTR) $\approx$1.7 cm^3 m^{-2} day^{-1} bar^{-1} at 75% relative humidity). The coating not only decreases gas permeability through the films but also minimizes the sensitivity of performance to humidity levels. The clay-coated nanocomposite films outperformed various commercial polymers and are comparable to high-performance packaging films in terms of oxygen barrier properties. Further, the coating improved the mechanical properties of the films rendering them a prospective packaging material. These biodegradable, high-barrier and mechanically robust films are a promising advance in the field of sustainable packaging.

A. Venkateshaiah, S. Wacławek, M. Černík, V. V. T. Padil
Institute for Nanomaterials
Advanced Technologies and Innovation (CXI)
Technical University of Liberec (TUL)
Studentská 1402/2, Liberec 1 461 17, Czech Republic
E-mail: vinod.padil@tul.cz
R. L. Timmins
Inorganic Chemistry I
University of Bayreuth
Universitttsstraße 30, Bayreuth 95447, Germany
E. Sehl, S. Agarwal
Macromolecular Chemistry II
University of Bayreuth
Universitätsstraße 30, Bayreuth 95447, Germany
E-mail: agarwal@uni-bayreuth.de

The ORCID identification number(s) for the author(s) of this article can be found under https://doi.org/10.1002/mame.202200008

1. Introduction

Synthetic, conventional plastics used in single-use applications such as food packaging, grocery bags, disposable utensils, and beverage containers are accumulating in landfills, posing a severe environmental threat. These materials, made of polymer multilayers, are often lined with aluminum and contaminated with food; thus are not recyclable.[1] Plastic debris has become ubiquitous in the ecosystem and has even littered all the major ocean basins, rivers, and water bodies.[2] Microplastics, a form of plastic debris, when ingested, might threaten wildlife and marine life by obstructing their digestive tracts. They can later be translocated to the circulatory system and other tissues and transferred from prey to predator through the food chain.[3] These plastic wastes can be eliminated by utilizing extreme thermal processes like combustion and pyrolysis. However, these processes release greenhouse gases, which can be detrimental to the environment. These disastrous consequences can thus be mitigated by using biomass-derived materials that degrade via naturally occurring pathways.[4] Currently, there aren't any completely biodegradable, biomass-derived packaging materials that satisfy the barrier and mechanical property requirements while still being economically viable.[5] As a result, researchers are looking for a bio-sourced, biodegradable material that can replace traditional plastics in single-use applications.[6–9]

Bio-sourced polysaccharides, which are one of the most available raw materials in nature, have sparked a lot of interest in replacing single-use plastics. Their abundant availability, combined with their biodegradability, nontoxicity, and biocompatibility, can solve the aforementioned issue. Tree gums are one such polysaccharide that has recently gained interest as a packaging substitute.[10–12] The potential of tree gums like Arabic, Karaya, Kondagogu, Cashew, and Tragacanth to form films appropriate for food packaging has been investigated.[13] Tree gums are high molecular weight polysaccharides exuded from plants/trees as a defense mechanism against mechanical injury, chemical injury, microbial/insect attacks, and water stress. This process is called gummosis, and the obtained exudates form gels or viscous solutions in their respective solvents. Hydrocolloids, or water-soluble gums, have found applications in food, pharmaceutical,

biomedical and cosmetic industries owing to their abundance, low cost, biocompatibility, nontoxicity, gelling ability, chemical inertness, water binding potential, and emulsion stabilization ability.[14,15] Gum kondagogu is a polysaccharide obtained from the exudates of *Cochlospermum Gossypium*, a native Indian tree. Kondagogu has a high acidic sugar content, with glucuronic and galacturonic acids accounting for 52% of total carbohydrates, along with neutral sugars including glucose, rhamnose, galactose, and arabinose.[16] The structural, physicochemical, morphological, rheological. and compositional characteristics of kondagogu have been studied and reported.[17–22] The toxicological studies on kondagogu revealed that it is non-toxic, making it a suitable material for fabricating packaging films.[23] The use of kondagogu to fabricate packaging films is minimal and yet to be thoroughly investigated. The films made from kondagogu, like most polysaccharide films, have intrinsic limitations that need to be addressed, such as high hydrophilicity, poor mechanical properties, and barrier properties. This could be overcome by combining kondagogu with different biopolymers,[24] incorporating nanoparticles,[25] and chemical modification.[26]

We recently reported the use of dodecenylsuccinic anhydride (DDSA) modified kondagogu and cellulose nanofibers to fabricate packaging films.[26] The chemical modification was clearly effective in overcoming the kondagogu films' intrinsic brittleness moisture sensitivity while retaining biodegradability. DDSA's long chain alkenyl groups function as an internal plasticizer, imparting stearic hindrance to polysaccharide chains while inhibiting chain aggregation and hydrogen bond formation. This material's mechanical and barrier properties improved significantly when combined with cellulose nanofibers. However, even with the hydrophobic modification, the barrier properties of the films decreased exponentially at higher relative humidity (RH) levels. Despite the modification, kondagogu and cellulose nanofibers retain a certain affinity to moisture. This affinity causes self-association of water molecules which has plasticizing and/or swelling effect on the film. Due to the moisture-induced changes in polysaccharide chains' conformation, crystallinity, and mobility, these effects become much more pronounced at higher RH.[25]

Single-layer biopolymer films seldom fulfill the industrial criteria for barrier characteristics specified for packaging, thus necessitating modifications. Biopolymer films' barrier properties have been enhanced by chemical and physical crosslinking and surface treatments such as grafting and coating.[28,29] These approaches have been proven to enhance the barrier characteristics of biopolymers, and they are frequently employed in conjugation to meet commercial requirements. Coating of biopolymer films to improve barrier properties has recently gained significant attention.[30–33] Studies on coating biopolymer films with graphene oxide,[34] nanocellulose,[31] chitin nanofibers,[35] whey protein,[36] polylactic acid,[37] waxes,[38] and inorganic materials[39] have been reported. Inorganic two-dimensional (2D) nanosheets are proven to be impervious to gas molecules.[40] Coating these inorganic dispersions onto biopolymer films yields a high aspect ratio lamellar structure. This creates a tortuous path for the gaseous molecular diffusion across polymeric materials, improving barrier characteristics. Breu and coworkers have proven this by using synthetic layered silicates like sodium

hectorite (NaHec), possessing a high aspect ratio, cation exchange capability, and osmotic swelling properties to improve the gas barrier properties of polymer films.[41] Further, Habel et al. coated poly L-lactide (PLA) films with waterborne dispersions of NaHec and obtained biopolymer films with exceptional barrier properties.[42] The authors observed that the clay coating improved the oxygen barrier properties by a factor of four while having no negative impact on the biodegradability of the PLA films. This improvement in the oxygen barrier was observed even at elevated RH, suggesting that the NaHec nanoparticles limit the diffusion of oxygen molecules through the film via the tortuous path mechanism regardless of RH. This would aid in improving the barrier qualities of biobased polymer films, which are strongly reliant on humidity conditions. In addition to excellent oxygen barrier properties, these waterborne clay dispersion coatings can even provide a water vapor barrier in a scalable manner. Based on this concept, we spray-coated NaHec onto hydrophobically modified kondagogu nanocomposites to produce high-barrier, biodegradable films with improved mechanical properties. The effects of cellulose nanofiber incorporation and NaHec coating on the barrier properties of the kondagogu films were analyzed at different humidity conditions. The resulting films had barrier properties that were superior to most conventional plastics.
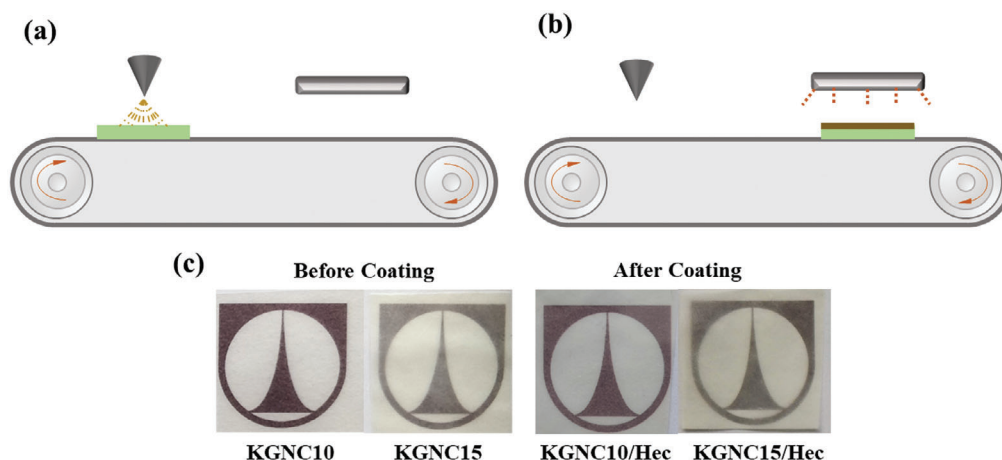
## 2. Results and Discussion

2.1. Fabrication of KGNC/Hec Films

Our team has recently reported the detailed synthesis procedures and extensive characterization of DDSA modified kondagogu and cellulose nanofiber incorporated DDSA modified kondagogu (KGNC) films.[24] We selected KGNC films with 10% and 15% cellulose nanofiber (CNF) in this study because they had the best mechanical and barrier properties[26] and would be ideal for studying the combined effect of CNF incorporation and clay coating. Herein, we have used a melt-processed synthetic sodium hectorite (NaHec, $[Na_{0.5}]^{inter}[Mg_{2.5}Li_{0.5}]^{oct}[Si_4]^{tet}O_{10}F_2$) clay that can gently, osmotically delaminate into a high-aspect-ratio ($\approx 20\,000$) single layers when dispersed in water, without the need for ultrasonication. This enables uniform non-isotropic, nematic phases in the dispersion. A high barrier layer was created on the films by spray coating a 0.25 wt.% aqueous dispersion on a KGNC substrate (**Figure 1**). A total of 200 spraying/drying cycles were used to coat KGNC films with NaHec suspension to obtain the desired thickness of 3 μm. The suspension layer added in a single spraying process had a thickness of ≈ 1.5 μm, which corresponded to a dry film thickness of ≈ 20 nm. After 200 cycles, the final coating layer thickness was measured to be 3.144 ± 0.193 μm (ImageJ). The coatings were stable, and no loose powder was observed while handling the films. A slight decrease in transparency of the films was observed after NaHec coating (Figure 1c; Table S1, Supporting Information).

2.2. SEM and TEM analysis of the KGNC/Hec films

The surface morphology of the NaHec coated 15 wt.% cellulose nanofiber incorporated DDSA modified kondagogu (KGNC15)

**ADVANCED
SCIENCE NEWS**

www.advancedsciencenews.com

[M] acro-
molecular

Materials and Engineering

www.mame-journal.de

Figure 1. Schematic representation of the NaHec automated a) spray coating, b) drying process, and c) digital images of KGNC films before and after coating.
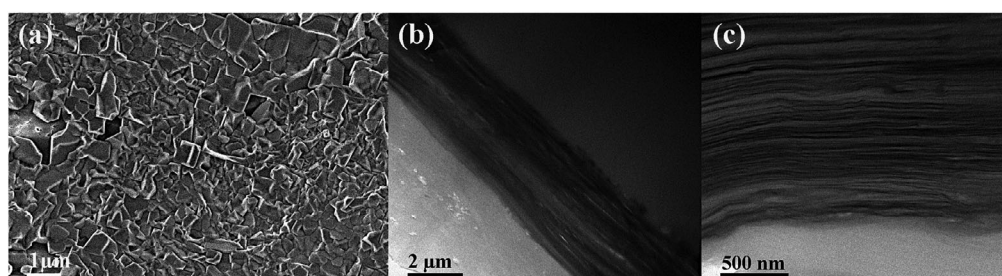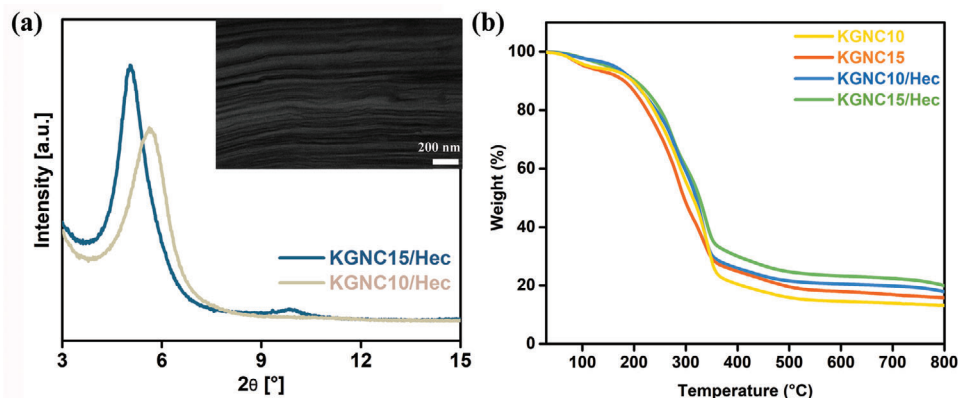

Figure 2. Morphology analysis of KGNC15/Hec film surface by a) SEM image and cross-section by b,c) TEM images.

film was observed by scanning electron microscopy (SEM) (**Figure** 2a). The image revealed the rough surface of the film with high aspect ratio clay nanoplatelets covering the film surface completely. Unlike the KGNC films, no cellulose nanofibers were observed on the film surface, suggesting that the NaHec suspension was evenly coated (Figure S2, Supporting Information; Figure 2a). The cross-sectional surface observed by transmission electron microscopy (TEM) analysis revealed a highly ordered orientation of clay nanoplatelets on the KGNC15 film substrate (Figure 2b,c). The light grey part is the KGNC film substrate, and the layered structure on top of it is the NaHec coating. Upon spraying the dilute dispersion of highly anisotropic NaHec platelets, the clay particles collide with the KGNC film substrate at high speeds. As a result of the collision, the droplets disperse on the film surface, while the 2D clay nanoplatelets tend to kinetically arrange themselves into dense parallel positions to the film surface.[43] Furthermore, a thin liquid suspension film forms on the surface after each spraying phase, allowing for ample mobility of the particles. With 90 sec drying time, the nanoplatelets have enough time to align themselves in the most favorable parallel position. This could be clearly seen by the TEM images, wherein highly delaminated NaHec structures are arranged equidistantly on the film surface. This highly ordered parallel orientation of NaHec platelets ensues a tortuous pathway for gas diffusion, resulting in enhanced barrier properties.

2.3. Crystallinity and Thermal Analysis of the Films

X-ray diffraction (XRD) analysis revealed the perfectly aligned structure of the NaHec coatings on the KGNC substrates. Breu et al. have studied and reported the crystallographic data of NaHec in thorough detail.[44,45] **Figure 3**a shows a sharp diffraction peak at $2\theta_{001} = 5.6°$ for KGNC10/Hec and $5.05°$ for KGNC15/Hec, corresponding to monohydrated sodium cations in the interlayer space with a normal d-spacing of 1.67 and 1.72 nm, respectively. The 1D crystalline nanocomposite coatings have 0.96 nm thick NaHec platelets separated by 0.71 nm and 0.76 nm of PVA matrix for KGNC10/Hec and KGNC15/Hec, respectively. This implies that the nanocomposite coating is biphasic, predominantly consisting of 1D crystalline layers of clay domains intercalated by a secondary minor polyvinyl alcohol (PVA) phase (Figure 3a inset). In the case of KGNC15/Hec, a small diffraction peak corresponding to the second-order of the 1D crystal was also observed at $2\theta_{001} = 9.87°$. Since the PVA volume in the interlayer spacing is small, their influence on the bulk properties can be negligible. Further, the thermogravimetric analysis (TGA) analysis of the samples was carried out and depicted in Figure 3b. All films exhibit an initial weight loss below 200 °C as a result of loss of adsorbed moisture. The breaking of ester bonds between kondagogu and DDSA at 200 °C causes the release of alkenyl chains, resulting in weight loss,[22] followed by the degradation of gum polysaccharide chains above 250 °C.[21] From Fig-

ADVANCED SCIENCE NEWS
www.advancedsciencenews.com

[M]acro-molecular
Materials and Engineering
www.mame-journal.de

Figure 3. a) XRD pattern of the NaHec coating on KGNC film substrates. The inset is a TEM image of the NaHec coating with highly oriented PVA intercalated NaHec platelets on the KGNC15 substrate. b) TGA curves of uncoated and coated KGNC films.
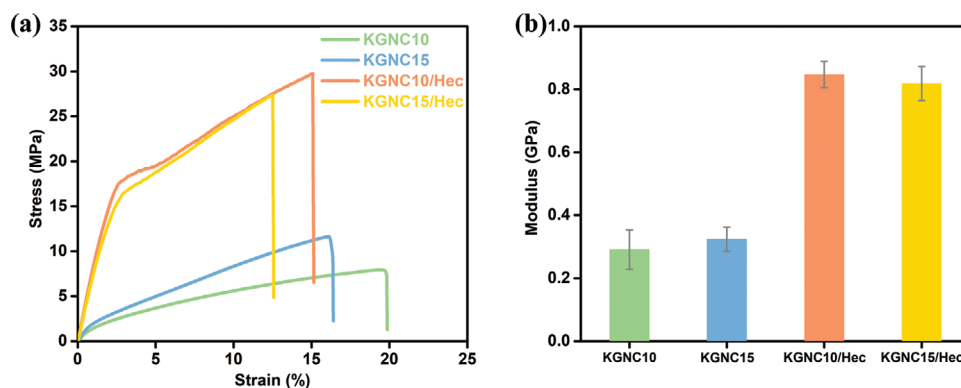
Figure 4. a) Stress-strain curves and b) Modulus of NaHec coated and uncoated films.

ure 3b, it can be seen that the NaHec coating has no significant effect on the thermal stability of the films. However, the KGNC/Hec samples show an increased leftover mass than the KGNC film samples. This increased leftover mass can be attributed to NaHec particles, which do not decompose below 800 °C.[46]

2.4. Mechanical Properties of the Films

The mechanical performance of the uncoated and NaHec coated KGNC films were analyzed and presented in **Figure 4** and Table S2 (Supporting Information). The effect of NaHec coating on the mechanical properties of the films was determined by evaluating their tensile strength (TS), elongation at break (ϵ), and modulus. From Figure 4a, it is evident that the CNF loading increases the TS of the films. This increase in TS arises from the secondary interactions between the hydroxyl groups of CNFs and the matrix via hydrogen bonding. This enables a stiff network between the polysaccharide chains and the CNFs; as a result, a decrease in the ϵ was observed. NaHec coating significantly enhanced the tensile strength of the films. A three-fold increase in the tensile strength of the films was observed after coating. Additionally, the NaHec layer on the KGNC films serves as a stress transfer agent, increasing the tensile strength of composite films in general. However, unlike uncoated samples, KGNC10/Hec with lower CNF loading exhibits higher TS values than KGNC15/Hec. This could be due

to the aggregation of CNF at higher loadings.[22] These aggregates may interfere with and inhibit the interactions between the Hec coating and the film, resulting in lower TS values. The coating further contributes to the stiffness of the films, which was evident by the decrease in the elongation at break values. A similar effect has been observed in other clay-biopolymer nanocomposites and coatings.[47–49] In comparison to uncoated films, the modulus of the NaHec coated films increased by around 200%. This emphasizes the synergistic effect the clay coating has on the bio-nanocomposite films. Further, the films were subjected to repetitive bending deformation up to 50 times, and no delamination of the NaHec coating was observed. This suggests good compatibility between NaHec coating and KGNC films. Hydrophilic clay nanoparticles have been known to show affinity toward biopolymers like carrageenan,[50] karaya,[47] agar,[51] and proteins.[52]

2.5. Barrier Properties of the Films

The shelf life of products is primarily determined by the barrier properties of their packaging material, and hence high barrier properties are required in the packaging materials.[53] Pristine biopolymer films have inferior barrier properties and thus would almost certainly need to be compounded with fillers that enhance barrier properties to gain prominence in the high-performance packaging industry.[54] Since ISO 14663-2 specifies 65% RH as
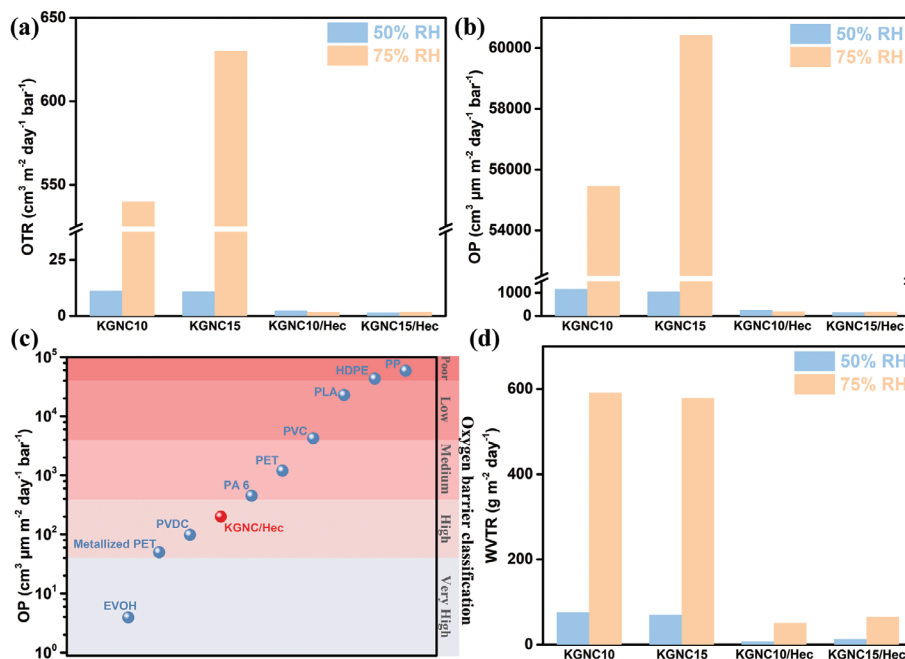
Figure 5. Barrier properties of the uncoated and NaHec coated KGNC films a) OTR, b) OP, c) comparison of OP values with common packaging materials, d) WVTR. EVOH, ethylene vinyl alcohol[55]; HDPE, high-density polyethylene[56]; PA 6, polyamide 6[55]; PET, polyethylene terephthalate[42]; PLA, polylactic acid[42]; PP, polypropylene[55]; PVC, polyvinyl chloride[55]; PVDC, polyvinylidene chloride[55]; Metallized PET, aluminum coated polyethylene terephthalate.[56]

a standard measurement for PVA, we rely on a spectrum of RH (50% and 75% RH) enclosing this standard.

The KGNC films containing CNF exhibited good barrier properties at 50% RH; however, at 75% RH, an exponential drop in the barrier properties was observed (**Figure 5** and Table S3, Supporting Information). This poor barrier performance at high RH could be due to the affinity of kondagogu and CNF to moisture leading to swelling and plasticization. As a result, the absorbed water molecules increase the polysaccharide chain mobility, thereby breaking the barrier structure and allowing the gas molecules to diffuse through the film.[24] Due to their low barrier properties at high RH volumes, they may not be suitable for long-term storage in humid environments. The clay coating has been known to minimize not only the biopolymer film's permeability but also its susceptibility to water vapor concentrations. This ability of NaHec has been studied and established on several other polymer matrices.[42,43,57] The nanocomposite coating's lamellar structure is comparable to natural nacre with low free inner volume arising from the large aspect ratio of the NaHec platelets. This, along with CNF and the high filler content, is beneficial in creating a tortuous path for gas diffusion, thereby enhancing the barrier properties (Figure S2, Supporting Information). Building on this idea, NaHec clay nanoplatelets delaminated in PVA solution were coated onto KGNC films. Prior to measuring the oxygen transmission rate (OTR) and water vapour transmission rate (WVTR) values, all films were carefully conditioned at room temperature and at different RH levels (50% and 75%). At 50% RH, the KGNC/Hec films with ≈3 μm NaHec coating demonstrate exceptional barrier properties (Figure 5). The OTR values of the films were as low as ≈2 cm³ m⁻² day⁻¹ bar⁻¹, a five-fold decrease from the uncoated films (Figure 5a). Further, as hypoth-

esized, increasing the RH to 75% had a negligible effect on the OTR values. The uncoated KGNC10 and KGNC15 films exhibited OTR values in the range of 540 and 630 cm³ m⁻² day⁻¹ bar⁻¹, respectively. Upon coating the films with NaHec dispersion, the OTR values decrease by more than two orders of magnitude with a >99% decrease in oxygen transmission. However, for a more accurate comparison of these findings, the transmission rates are converted into permeabilities as the thickness of the films has been known to influence the transmission rates significantly. Oxygen permeability (OP) can be defined as the rate of oxygen transmitted per unit thickness of the film. Based on these findings, the KGNC/Hec films clearly outperform the most widely used non-biodegradable traditional plastic packaging films, several coated and multilayered biopolymer films and are comparable to high-performance packaging materials like polyvinylidene chloride (PVDC) and aluminum-coated polyethylene terephthalate (PET) films (Figure 5c; Table S4, Supporting Information). The tortuous diffusion path formed by high aspect ratio NaHec platelets may be directly responsible for this improved oxygen barrier property. This is because in the absence of NaHec, PVA coatings have been shown to have significantly lower permeability reductions, and their efficiency is extremely sensitive to moisture.[42] Further, the WVTR of the coated and uncoated films were evaluated and depicted in Figure 5d. The same trend observed in OTR holds well for the WVTR values of the coated and uncoated films. The NaHec coating significantly reduced water vapor transmission through the films. Even at an elevated RH of 75%, the WVTR values are reduced by a factor of 9, further emphasizing the lower moisture sensitivity arising from the high aspect ratio NaHec coating. Given the moisture sensitivity of kondagogu and CNF, as well as the water-based formulation of KGNC
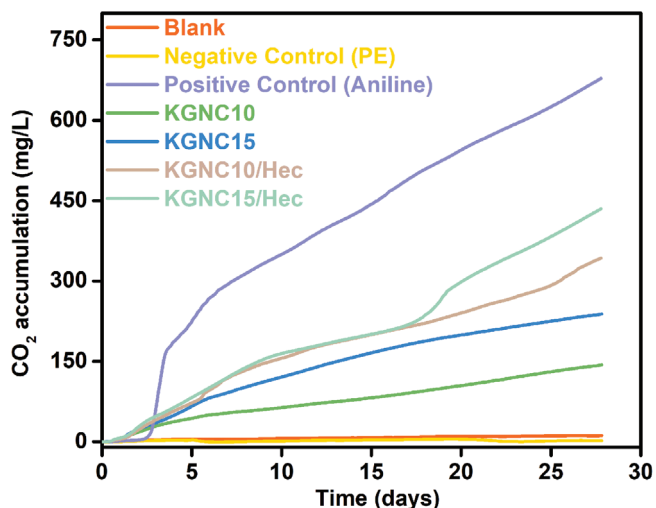
Figure 6. CO_2 accumulation as a function of time of KGNC films.

films and the NaHec coatings, the significant reduction in WVTR values was noteworthy.

2.6. Biodegradability of the Films

The biodegradation of the samples was carried out in an aqueous medium under aerobic conditions with polyethylene (PE) as negative control and aniline as a positive control. The cumulative CO_2 of each test sample was determined and plotted as a function of time to analyze the biodegradation rate (**Figure 6**). The microbes consume oxygen and degrade the polysaccharide chains generating carbon dioxide. As a result, monitoring CO_2 buildup in the cell could offer information on the biodegradation rate of samples. All the tested biopolymer film samples exhibit biodegradability, and the biodegradation increases with the increase in incubation time. The CO_2 accumulation trend suggests that the biodegradation rate increases quickly at the beginning of the test, which seems to level off as the test proceeds. This could be attributed to the increased availability of organic resources for microbial assimilation, resulting in an increase in the number of microbial colonies. As the test progresses, these resources get exhausted, slowing the rate of biodegradation. From the results, it was evident that the rate of degradation of coated samples was higher than the uncoated samples. The improved rate of biodegradation could be due to the ability of the clay to promote hydrolytic degradation. Furthermore, soaking the film in water causes the clay to swell, resulting in fragmentation of the film, which increases the surface area, thereby improving the biodegradation rate.[58] This acceleration of biodegradability in the presence of clay nanoparticles has been observed in both conventional and biobased polymers.[59–63]

3. Conclusions

High barrier, biodegradable packaging films based on gum kondagogu were prepared by spray coating kondagogu/CNF nanocomposite films with a waterborne dispersion of PVA and

NaHec. The entire film fabrication and coating process are water-based, making it environmentally friendly. The exfoliated NaHec platelets formed a thin layer (≈3 µm) of highly ordered nacre-like structure on the KGNC films. The coating improved the mechanical properties of the material, as shown by the increased tensile strength and modulus. Coating the films resulted in a threefold increase in tensile strength and a 200% improvement in modulus. The obtained flexible packaging films exhibit high barrier performance superior to many traditional plastics. The clay layer formed a tortuous path for gas molecules to diffuse across, dramatically limiting their permeability. The coated films had OTR values of ≈2 cm³ m⁻² day⁻¹ bar⁻¹, a fivefold improvement over the uncoated films. The enhanced barrier properties are negligibly affected by the increase in RH, as evidenced by a more than 99% decrease in oxygen transmission rates and a reduction in water vapor transmission rate by a factor of 9, even at 75% RH. Thus, KGNC/Hec films can be suitable for long-term packaging even in highly humid conditions.

4. Experimental Section

Materials: Gum Kondagogu (Grijian Cooperative society, Hyderabad, India) was purified and deacetylated using the methods we previously reported.[24] Melt synthesis was used to synthesize sodium hectorite (Na-Hec) $[Na_{0.5}]^{inter}[Mg_{2.5}Li_{0.5}]^{oct}[Si_4]^{tet}O_{10}F_2$, following a process described in the literature.[47] The material had a 1.27 mmol g⁻¹ cation exchange capacity (CEC) and a high aspect ratio >20 000. Cellulose nanofiber (CNF, $d = 10$–20 nm, $l = 2$–3 µm) was purchased from Nanografi co. Ltd., Germany. Hydrochloric acid, Sodium hydroxide, DDSA, Polyvinyl alcohol (PVA, Mowiol 20–98 Mw ≈125 000), ethanol absolute, glycerol, glutaraldehyde, cyclohexane (≥99%), and other analytical-grade chemicals were procured from Merck company.

DDSA Modification of Kondagogu and Fabrication of Nanocomposite Films: Chemical modification of kondagogu and film fabrication were carried out using the methods we recently reported.[24] Briefly, DDSA (30 wt.% of kondagogu, 30 mL) solution of absolute ethanol was slowly added to deacetylated kondagogu aqueous solution (2 g in 100 mL) at a pH of 8.5. After 7 h at constant pH of 8.5, 5% HCl was added to stop the reaction, and the product was purified by dialysis for 7 days against distilled water. The lyophilized product was further purified by Soxhlet extraction with cyclohexane and dried overnight in an oven at 60 °C.

CNF reinforced gum films were prepared by dispersing CNF (10 and 15 wt.% of gum) in distilled water for 3 min at 12 000 rpm using a homogenizer. 2 w/v% of modified kondagogu gum was mixed with the CNF dispersion at 70 °C to ensure complete dissolution. Subsequently, glycerol (30 w/w%) was added as a plasticizer, followed by a few drops of 1 M HCl to achieve a pH of 3, and glutaraldehyde (10 w/w%) was added as a crosslinker. After 1 h of stirring to enable homogeneous mixing, the solutions were cast into Petri dishes and dried for 12 h in an oven at 60 °C. The DDSA modified kondagogu films containing 10 and 15% cellulose nanofibers were denoted as KGNC10 and KGNC15, respectively.

NaHec Clay Coating of Films: Delamination of dry NaHec (3 wt.%) was done in double-distilled water and allowed to mix for a week in an overhead mixer. This was added dropwise into PVA (5 wt.%) solution, and the total solid content was adjusted to 0.25% (50 wt.% NaHec, 50 wt.% PVA) using double distilled water, and the dispersion was mixed overnight. The dispersion was transferred to a speed mixer (Hauschild & Co. KG) to enhance the dispersion quality and eliminate gas bubbles under a vacuum just before coating. The dispersion was then transferred to a completely automated spray coating system (SATA 4000 LAB HVLP 1.0 mm spray gun, SATA GmbH & Co. KG, Germany). The obtained suspension was sprayed on the dry KGNC film substrate (4 bar, 1 mL s⁻¹) attached to a conveyor belt by means of a stationary airbrush (Figure 1a). The sample was then dried for 90 s under an IR lamp at 40 °C (Figure 1b) for each spray cycle (a total of 200 cycles). The films were then dried in an oven at 40 °C for 48 h

to ensure complete water removal. KGNC10/Hec and KGNC15/Hec were the designations for the coated KGNC10 and KGNC15 films, respectively.

Characterization Techniques: The surface morphology of the films was studied using a scanning electron microscope (SEM, UHR FE-SEM Carl Zeiss ULTRA Plus, Germany) with an acceleration voltage of 0.5–2.5 kV. Transmission electron microscopy (TEM) images were obtained on JEM-2200 FS (JEOL GmbH, Germany). An Ion Slicer EM09100IS (JEOL GmbH, Germany) was used to prepare thin cross-sections of the nanocomposite films with coating. A Jasco V630 UV–Vis spectrophotometer was used to determine the transparency of the films. X-ray diffraction (XRD) analysis was carried out on a Bragg-Bertano type diffractometer (Empyrean, Malvern Panalytical BV, The Netherlands) equipped with a Pixel-1D detector using nickel filtered Cu-Kα radiation (λ = 1.54187 Å). A Thermogravimetric analyzer (TGA-4000, PerkinElmer, USA) was used to determine the films' thermal stability. The samples (5 mg) were analyzed in an inert atmosphere with a nitrogen flow rate of 50 mL min^{-1}. The analysis was done at a temperature range of 30–800 °C with a heating rate of 10 °C min^{-1}. Stress–strain analysis on a Zwick/Roell BT1-FR 0.5TND14 was used to evaluate the mechanical properties of the films. The samples were cut into 3 mm × 30 mm dimensions and conditioned at 20°C for 24 h prior to testing. A Mitutoyo 293–805 optical micrometer with a precision of 1 μm was used to measure the thickness of each specimen. The width of the specimens was measured using a Zeiss digital microscope, Smartzoom 5 equipped with a Zeiss PlanApo D 1.6x/0.1 FWD 36 mm objective (36 × magnification) with a precision of ≈3 μm (2 pixels), taking the average of theww different positions in the gauge area as the final width. The samples were tested at a tensile speed of 5 mm min^{-1} with a pristine gauge length of 10 mm. The slope of the linear region of the stress-strain curves was used to calculate the elastic modulus. The analysis was performed on at least ten specimens, and the statistical average is reported as a result. Mocon OX-TRAN 2/21 instrument was used in the measurement of oxygen transmission rates (OTR) with a lower detection limit of 0.05 cm^3 m^{-2} day^{-1} bar^{-1}. As a carrier gas, a combination of 98% nitrogen and 2% hydrogen was used, with pure oxygen (>99.95%, Linde Sauerstoff 3.5) as the permeant gas. The tests were performed at a temperature of 23°C and relative humidity of 50% and 75%. Mocon PERMATRAN-W 3/33 instrument with a lower detection limit of 0.5 g m^{-2} day^{-1} was used to determine the water vapor transmission rates (WVTR). The analysis was performed at 23°C and relative humidity of 50% and 75%.

The materials were evaluated for biodegradability under aerobic circumstances according to European standard technique based on ISO 14 851:1999. As an inoculum, 4.7 g L^{-1} activated sludge from a wastewater treatment plant (WWTP; Liberec, Czech Republic) containing about 100 000 CFU mL^{-1} was utilized. The inorganic medium was prepared by a mixture of four different solutions. Solution 1 had a mixture of 8.5 g L^{-1} of KH$_2$PO$_4$, 21.75 g L^{-1} of K$_2$HPO$_4$, 33.4 g L^{-1} of Na$_2$HPO$_4$.2H$_2$O, and 0.5 g L^{-1} of NH$_4$Cl measuring a pH of 7.4; Solution 2 contained 22.5 g L^{-1} of MgSO$_4$.7H$_2$O; solution 3 contained 36.4 g L^{-1} of CaCl$_2$.2H$_2$O; solution 4 contained 0.25 g L^{-1} of FeCl$_3$.6H$_2$O. The medium was prepared by adding 10 mL of solution 1 to 500 mL of distilled water along with 1 mL each of solution 2–4 and made up to 1000 mL. Pre-weighed samples (50 mg) were added to the biological mixture of 95 mL of inorganic medium and 5 mL of inoculum, then dosing the mixture into a 250 mL respiration cell and starting the test immediately for 28 days. At the same concentration, activated sludge containing no organics was utilized as a blank. A Micro-Oxymax respirometer (Columbus Instruments International, USA) with a paramagnetic oxygen sensor was used for measurements.

Supporting Information

Supporting Information is available from the Wiley Online Library or from the author.

Acknowledgements

Conflict of Interest

The authors declare no conflict of interest.

Data Availability Statement

The data that support the findings of this study are available in the supplementary material of this article.

Keywords

[1] R. Geyer, J. R. Jambeck, K. L. Law, *Sci. Adv.* **2017**, *3*, e1700782.

[2] A. Chamas, H. Moon, J. Zheng, Y. Qiu, T. Tabassum, J. H. Jang, M. Abu-Omar, S. L. Scott, S. Suh, *ACS Sustainable Chem. Eng.* **2020**, *8*, 3494.

[3] M. N. Issac, B. Kandasubramanian, *Environ. Sci. Pollut. Res.* **2021**, *28*, 19544.

[4] S. Singha, M. Mahmutovic, C. Zamalloa, L. Stragier, W. Verstraete, A. J. Svagan, O. Das, M. S. Hedenqvist, *ACS Sustainable Chem. Eng.* **2021**, *9*, 6337.

[5] Z. Yu, Y. Ji, V. Bourg, M. Bilgen, J. C. Meredith, *Emergent Mater.* **2020**, *3*, 919.

[6] L. S. F. Leite, C. Pham, S. Bilatto, H. M. C. Azeredo, E. D. Cranston, F. K. Moreira, L. H. C. Mattoso, J. Bras, *ACS Sustainable Chem. Eng.* **2021**, *9*, 8539.

[7] L. Guo, T. Qiang, Y. Ma, L. Ren, C. Zhu, *ACS Sustainable Chem. Eng.* **2021**, *9*, 8393.

[8] Y. Qiu, J. Fu, B. Sun, X. Ma, *e-Polymers* **2021**, *21*, 072.

[9] X.u Yan, W. Zhou, X. Ma, B. Sun, *e-Polymers* **2021**, *21*, 038.

[10] C. Zhang, Y. Zhang, R. Cha, K. Long, J. Li, X. Jiang, *ACS Sustainable Chem. Eng.* **2019**, *7*, 15404.

[11] Q. Ma, L. Cao, T. Liang, J. Li, L. A. Lucia, L. Wang, *ACS Sustainable Chem. Eng.* **2018**, *6*, 8926.

[12] V. V. T. Padil, C. Senan, S. Wacławek, M. Černík, S. Agarwal, R. S. Varma, *ACS Sustainable Chem. Eng.* **2019**, *7*, 5900.

[13] A. Khezerlou, H. Zolfaghari, S. A. Banihashemi, S. Forghani, A. Ehsani, *Polym. Adv. Technol.* **2021**, *32*, 2306.

[14] M. S. Amiri, V. Mohammadzadeh, M. E. T. Yazdi, M. Barani, A. Rahdar, G. Z. Kyzas, *Molecules* **2021**, *26*, 1770.

[15] S. Barak, D. Mudgil, S. Taneja, *J. Sci. Food Agric.* **2020**, *100*, 2828.

[16] Venkateshaiah, Silvestri, Ramakrishnan, Wacławek, Padil, Černík, Varma, *Molecules* **2019**, *24*, 3643.

[17] B. Janaki, R. B. Sashidhar, *Food Chem.* **1998**, *61*, 231.

[18] V. T. P. Vinod, R. B. Sashidhar, *Food Chem.* **2009**, *116*, 686.

[19] V. T. P. Vinod, R. B. Sashidhar, K. I. Suresh, B. Rama Rao, U. V. R. Vijaya Saradhi, T. Prabhakar Rao, *Food Hydrocoll* **2008**, *22*, 899.

[20] V. T. P. Vinod, R. B. Sashidhar, V. U. M. Sarma, U. V. R. Vijaya Saradhi, *J. Agric. Food Chem.* **2008**, *56*, 2199.

[21] V. T. P. Vinod, R. B. Sashidhar, V. U. M. Sarma, S. S. Raju, *Food Chem.* **2010**, *123*, 57.

[22] V. T. P. Vinod, R. B. Sashidhar, *Indian J. Nat. Prod. Resour.* **2010**, *1*, 181.

[23] B. Janaki, R. B. Sashidhar, *Food Chem. Toxicol.* **2000**, *38*, 523.

[24] R. K. Ramakrishnan, S. Wacławek, M. Černík, V. V. T. Padil, *Int. J. Biol. Macromol.* **2021**, *177*, 526.

[25] A. Venkateshaiah, J. Y. Cheong, C. Habel, S. Wacławek, T. Lederer, M. Černík, I. - D. Kim, V. V. T. Padil, S. Agarwal, *ACS Appl. Nano Mater* **2020**, *3*, 633.

[26] A. Venkateshaiah, K. Havlíček, R. L. Timmins, M. Röhrl, S. Wacławek, N. H. A. Nguyen, M. Černík, V. V. T. Padil, S. Agarwal, *Carbohydr. Polym.* **2021**, *266*, 118126.

[27] M. Kurek, A. Guinault, A. Voilley, K. Galić, F. Debeaufort, *Food Chem.* **2014**, *144*, 9.

[28] A. M. Youssef, S. M. El-Sayed, *Carbohydr. Polym.* **2018**, *193*, 19.

[29] S. M. El-Sayed, H. S. El-Sayed, O. A. Ibrahim, A. M. Youssef, *Carbohydr. Polym.* **2020**, *239*, 116234.

[30] P. Tyagi, K. S. Salem, M. A. Hubbe, L. Pal, L. Pal, *Trends Food Sci. Technol.* **2021**, *115*, 461.

[31] P. Tyagi, L. A. Lucia, M. A. Hubbe, L. Pal, L. Pal, *Carbohydr. Polym.* **2019**, *206*, 281.

[32] V.u T. T. Thuy, L. T. Hao, H. Jeon, J. M.o Koo, J. Park, E. S. Lee, S. Y. Hwang, S. Choi, J. Park, D. X. Oh, *Green Chem.* **2021**, *23*, 2658.

[33] T. Zhang, Q. Yu, L. Fang, J. Wang, T. Wu, P. Song, *ACS Appl. Polym. Mater.* **2019**, *1*, 3470.

[34] C. Sharma, P. H. Manepalli, A. Thatte, S. Thomas, N. Kalarikkal, S. Alavi, *Colloid Polym. Sci.* **2017**, *295*, 1695.

[35] C. C. Satam, C. W. Irvin, A. W. Lang, J. C. R. Jallorina, M. L. Shofner, J. R. Reynolds, J. C. Meredith, *ACS Sustainable Chem. Eng.* **2018**, *6*, 10637.

[36] P. Cinelli, M. Schmid, E. Bugnicourt, J. Wildner, A. Bazzichi, I. Anguillesi, A. Lazzeri, *Polym. Degrad. Stab.* **2014**, *108*, 151.

[37] R. Koppolu, J. Lahti, T. Abitbol, A. Swerin, J. Kuusipalo, M. Toivakka, *ACS Appl. Mater. Interfaces* **2019**, *11*, 11920.

[38] M. O. Reis, J. B. Olivato, A. P. Bilck, J. Zanela, M. V. E. Grossmann, F. Yamashita, *Ind. Crops Prod.* **2018**, *112*, 481.

[39] J. Vartiainen, K. Rose, Y. Kusano, J. Mannila, L. Wikström, *J. Coatings Technol. Res. 2019 171* **2019**, *17*, 305.

[40] Y. Cui, S. Kumar, B. Rao Kona, D. Van Houcke, *RSC Adv.* **2015**, *5*, 63669.

[41] M. W. Möller, D. A. Kunz, T. Lunkenbein, S. Sommer, A. Nennemann, J. Breu, *Adv. Mater.* **2012**, *24*, 2142.

[42] C. Habel, M. Schöttle, M. Daab, N. J. Eichstaedt, D. Wagner, H. Bakhshi, S. Agarwal, M. A. Horn, J. Breu, *Macromol. Mater. Eng.* **2018**, *303*, 1800333.

[43] E. S. Tsurko, P. Feicht, C. Habel, T. Schilling, M. Daab, S. Rosenfeldt, J. Breu, *J. Memb. Sci.* **2017**, *540*, 212.

[44] H. Kalo, W. Milius, J. Breu, *RSC Adv.* **2012**, *2*, 8452.

[45] M. Stöter, D. A. Kunz, M. Schmidt, D. Hirsemann, H. Kalo, B. Putz, J. Senker, J. Breu, *Langmuir* **2013**, *29*, 1280.

[46] E. S. Tsurko, P. Feicht, F. Nehm, K. Ament, S. Rosenfeldt, I. Pietsch, K. Roschmann, H. Kalo, J. Breu, *Macromolecules* **2017**, *50*, 4344.

[47] T. L. Cao, K. B. Song, K. Bin Song, *Food Hydrocoll* **2019**, *89*, 453.

[48] J. Zhu, A. Kumar, P. Hu, C. Habel, J. Breu, S. Agarwal, *Glob. Challenges* **2020**, *4*, 2000030.

[49] J. Zhu, C. Habel, T. Schilling, A. Greiner, J. Breu, S. Agarwal, *Macromol. Mater. Eng.* **2019**, *304*, 1800779.

[50] M. J. Sanchis, M. Carsí, M. Culebras, C. M. Gómez, S. Rodriguez, F. G. Torres, *Carbohydr. Polym.* **2017**, *176*, 117.

[51] J. -. W. Rhim, S. -. B. Lee, S.-I.n Hong, *J. Food Sci.* **2011**, *76*, N40.

[52] J.i-H. Lee, N. -. B. Song, W. -. S. Jo, K. B. Song, K. Bin Song, *Int. J. Food Sci. Technol.* **2014**, *49*, 1869.

[53] E. Ruggeri, D. Kim, Y. Cao, S. Farè, L. De Nardo, B. Marelli, *ACS Sustainable Chem. Eng.* **2020**, *8*, 14312.

[54] S. Davoodi, S. M. Davachi, A. Ghorbani Golkhajeh, A. S. Shekarabi, A. Abbaspourrad, *ACS Sustainable Chem. Eng.* **2020**, *8*, 1487.

[55] J. Wang, D. J. Gardner, N. M. Stark, D. W. Bousfield, M. Tajvidi, Z. Cai, *ACS Sustainable Chem. Eng.* **2018**, *6*, 49.

[56] J. Lange, Y. Wyser, *Packag. Technol. Sci.* **2003**, *16*, 149.

[57] E. Doblhofer, J. Schmid, M. Rieß, M. Daab, M. Suntinger, C. Habel, H. Bargel, C. Hugenschmidt, S. Rosenfeldt, J. Breu, T. Scheibel, *ACS Appl. Mater. Interfaces* **2016**, *8*, 25535.

[58] R. L. Timmins, A. Kumar, M. Röhrl, K. Havlíček, S. Agarwal, J. Breu, *Macromol. Mater. Eng.* **2021**, 2100727.

[59] E. Chiellini, A. Corti, S. D'antone, R. Solaro, *Prog. Polym. Sci.* **2003**, *28*, 963.

[60] T. O. Kumanayaka, R. Parthasarathy, M. Jollands, *Polym. Degrad. Stab.* **2010**, *95*, 672.

[61] H. Qin, Z. Zhang, M. Feng, F. Gong, S. Zhang, M. Yang, *J. Polym. Sci. Part B Polym. Phys.* **2004**, *42*, 3006.

[62] S. Mohanty, S. K. Nayak, *J. Polym. Environ.* **2012**, *20*, 195.

[63] E. Castro-Aguirre, R. Auras, S. Selke, M. Rubino, T. Marsh, *Polymers (Basel)* **2018**, *10*, 202.